

## DIRECT NUMERICAL SIMULATION ON THE EFFECTS OF SLIP VELOCITY OF WAVY WALLS ON TURBULENT HEAT TRANSFER AND DRAG

**Atsushi Nishida**

Dept. of Mechanical and System Engineering,  
 Kyoto Institute of Technology  
 Sakyo-ku, Kyoto 606-8585, Japan  
 m3623039@edu.kit.ac.jp

**Kotaro Nakatsuji**

Dept. of Mechanical and System Engineering,  
 Kyoto Institute of Technology  
 Sakyo-ku, Kyoto 606-8585, Japan  
 M5623021@edu.kit.ac.jp

**Yoshimichi Hagiwara**

Dept. of Mechanical and System Engineering,  
 Kyoto Institute of Technology  
 Sakyo-ku, Kyoto 606-8585, Japan  
 yoshi@kit.ac.jp

### ABSTRACT

We have carried out direct numerical simulation on turbulent flow in a slippery wavy channel where heat transfer occurs. The amplitude of the channel wavy wall is 6 wall units and the local, instantaneous slip velocity is proportional to the velocity at an adjacent grid point to the wall. Two values proportional constants are used. The computational results show that the mean wall-shear stresses for the wavy walls do not depend on the slip velocity, and are much lower than those for a non-slip flat wall. This low wall-shear stress is due to the low gradient of mean velocity for the wavy walls. In addition, the mean Nusselt number for the wavy walls increases with an increase in the slip velocity. This increase in the Nusselt number is due to the decrease in the mean temperature gradient in the buffer region. This decrease in the temperature gradient is due to the gradient of turbulent heat flux in the region.

### INTRODUCTION

Convective heat transfer associated with turbulent wall-bound flow is seen in industrial equipment and heat exchangers. Thus, this convective heat transfer has been studied widely. Nevertheless, the demand for techniques for the elucidation, prediction and control of turbulent heat transfer is high. This is because the heat transfer is enhanced by turbulence and, at the same time, the frictional drag increases by the Reynolds analogy. It is very important for energy-saving to prevent an increase of the frictional drag while keeping effective heat transfer.

The present authors' research group has studied turbulent flows over wavy walls, and obtained the reduction of friction drag (Fujii et al., 2011). Furthermore, Akaiwa, Nishida and Hagiwara (2014) have studied drag reduction and heat transfer for turbulent flow in channels. They found that wavy walls, whose ratio of the amplitude to the wavelength was much lower than the critical value for the onset of re-circulating flow, can reduce frictional drag. They also found an increase in the Nusselt number.

However, the effects of slippery wavy walls on heat transfer were not discussed in detail.

The present study provides computational results for various slippery wavy surfaces. We carry out direct numerical simulation for turbulent flow and heat transfer in a channel with gentle two-dimensional wavy surfaces, and investigate the possibility of drag reduction and heat transfer enhancement. The slippery surface is realized by using a slip velocity at the wall. This study focuses on the elucidation of the effects of the difference in the slip velocity on the turbulent friction drag and turbulent heat transfer.

### COMPUTATIONAL METHODS

#### Computational domain

We dealt with turbulent flow in a domain between two wavy walls as shown in Figure 1. The walls have an identical, sinusoidal shape. The  $x^*$ -,  $y^*$ - and  $z$ -axes were positioned in the streamwise, vertical and transverse directions, respectively. The  $x$ -axis aligns with the streamwise direction along the wall and the  $y$ -axis is normal to the wall. The domain was converted to the computational domain, which was a rectangular box of  $2\pi h \times 2h \times \pi h$ , by using an unsteady generalized curvilinear coordinate system.

#### Governing equations

The equation of continuity, the Navier-Stokes equation, and the energy equation were solved.

$$\frac{1}{J} \frac{\partial(JU^j)}{\partial\xi^j} = 0 \quad (1)$$

$$\frac{\partial u_i}{\partial t} + U_k \frac{\partial u_i}{\partial \xi^k} = -\frac{1}{\rho} \frac{\partial \sigma_i}{\partial x_i} - \frac{\partial p}{\partial \xi^k} + \frac{\nu}{J} \frac{\partial}{\partial \xi^k} \left( J \frac{\partial \xi^k}{\partial x_m} \frac{\partial \xi^l}{\partial x_m} \frac{\partial u_i}{\partial \xi^l} \right) \quad (2)$$

$$\frac{\partial T}{\partial t} + U_k \frac{\partial T}{\partial \xi^k} = \frac{\alpha}{J} \frac{\partial}{\partial \xi^k} \left( J \frac{\partial \xi^k}{\partial x_m} \frac{\partial \xi^l}{\partial x_m} \frac{\partial T}{\partial \xi^l} \right) - \int \bar{u} dy \frac{q_w}{\rho C_p} \quad (3)$$

where:  $\zeta$  and  $U$  are the coordinate and velocity in the computational domain respectively;  $J$  is the Jacobian of the transformation;  $u$  is the velocity in the physical domain;  $p$  is the pressure;  $\rho$  is the density;  $\nu$  is the kinematic viscosity;  $T$  is the temperature;  $\alpha$  is the thermal diffusivity;  $\bar{u}$  is the mean velocity in the  $x$ -direction;  $C_p$  is the specific heat at constant pressure and  $q_w$  is the wall heat flux.

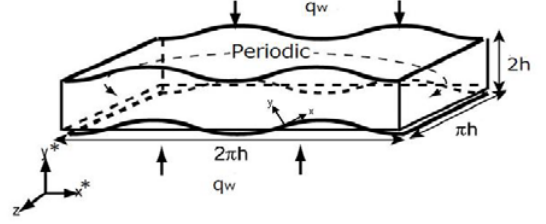


Fig. 1 Wavy wall domain.

### Schemes and grid arrangement

The governing equations were discretized with a collocated grid system. The velocity components, the pressure and temperature were defined at each grid point, while the product of the contravariant velocities and transformation Jacobian were defined at the midpoints between two neighboring grid points. The grid spacing was identical both in the  $x$ -direction and the  $z$ -direction. The spacing increased from the lower and upper walls in the  $\eta$  direction based on a hyperbolic tangent. The grid spacing was  $\Delta x^+ = 8.84$ ,  $\Delta y^+ = 0.66 - 9.09$  and  $\Delta z^+ = 4.42$  in the case of the flat wall. The grid resolution of the present study is sufficiently comparable to that of Kawamura et al ( $\Delta x^+ = 9$ ,  $\Delta y^+ = 0.40 - 11.5$  and  $\Delta z^+ = 4.5$ ) (Kawamura et al., 1998; 2000).

The 3rd-order accurate Runge-Kutta method was used for the time evolution. The 4th-order central difference scheme with the interpolating method for the collocated grid (Morinishi, 1996) was applied to the finite differencing of the convection terms of the NS equation. The 4th-order central difference scheme without the interpolation method was used to discretize the viscous term. The pressure Poisson equation was solved using the Fast Fourier Transform, the SOR method and the residual cutting method (Tamura et al., 1997). The methods are summarized in Table 1.

### Boundary conditions

The periodic boundary condition was applied for velocity and pressure in the  $x^+$  and  $z^+$  directions. The mean pressure gradient,  $-dp^+/dx^+$ , was equal to unity and was identical in each case.

A non-slip or slip boundary condition was adopted for the walls. In the case of the non-slip condition,  $u = v = w = 0$  at any moment at any location on the surface. In the case of the slip condition, the streamwise velocity was assumed to be proportional to the adjacent streamwise velocity,  $u = Bu_1$  and  $v = w = 0$  at any moment at any location on the surface of the lower wall.  $u_1$  is the streamwise velocity at the adjacent grid to the surface. The values of  $B$  was set equal to 0.50 and 0.25. The slip length was equal to 0.33 wall units and 0.165 wall units, respectively. The same conditions were used for the upper wall.

The temperature at the lower wall was determined by the following equation:

$$\frac{\theta_0}{\theta_\tau} = \frac{\theta_1}{\theta_\tau} - \frac{q_w}{\kappa} \frac{\Delta y_1}{2} = \theta_1^+ - \frac{u_\tau \Delta y_1}{2\nu} \frac{\nu}{\alpha} = \theta_1^+ - \text{Re}_\tau \text{Pr} \frac{\Delta y_1}{2h^+}, \quad (4)$$

Table 1 Computational condition and schemes.

	Grid	Collocated Grid	
		Grid number	128 × 64 × 128
Discretized	Grid resolution	$\Delta x^+ (= \Delta x u_t / \nu)$	8.84
		$\Delta y^+ (= \Delta y u_t / \nu)$	0.66 - 9.09
		$\Delta z^+ (= \Delta z u_t / \nu)$	4.42
	Time step $\Delta t^+ (= \Delta t u_t^2 / \nu)$	0.0090	
Schemes	Time evolution method	3rd-order accurate Runge-Kutta Method	
	Coupling Algorithm	Fractional Step Method (FFT&SOR&Residual Cutting Method)	
	Difference method	4th-order central difference	
Boundary condition	x, z - direction	Periodic	
	y - direction	Upper : non-slip or slip Lower : non-slip or slip	
Non - dimensional number	Reynolds number $\text{Re}_\tau (= u_\tau h / \nu)$	180	
	Prandtl number	2	

where  $\theta$  is the temperature difference,  $T_w - T$  ( $T_w$  is the wall temperature.).  $\theta_0$  ( $T_w - T_0$ , with  $T_0$  representing the temperature at a point inside the wall) is the temperature difference inside the wall, and  $\theta_1$  ( $T_w - T_1$ , with  $T_1$  representing the temperature at an adjacent point to the wall) is the temperature difference for the adjacent location.  $\Delta y_1/2$  is the distance between the wall and the adjacent point.  $\theta_\tau$  is the friction temperature, and  $u_\tau$  is the friction velocity.  $\kappa$  is thermal conductivity, and  $\nu$  is the kinematic viscosity.  $\text{Re}_\tau (= hu_\tau / \nu)$  is the friction Reynolds number.  $\text{Pr}$  is the Prandtl number. The same conditions were used for the upper wall.

### Initial conditions

A database made up of fully developed flow between two flat walls was adopted as the initial velocity field. The wavy wall was realized by increasing the amplitude linearly in the period of  $0 \leq t^+ \leq 36$ .

We used the empirical equation obtained by Kader (1981) for the initial mean temperature profile.

$$\bar{\theta}^+ = \frac{1}{0.47} \ln \left\{ Y(y^+) \right\} + \left( 3.85 \text{Pr}^{\frac{1}{3}} - 1.3 \right)^2 + 2.12 \ln(\text{Pr}) \quad (5)$$

$$Y(y^+) = \begin{cases} y^+ & (0 \leq y^+ \leq h^+) \\ 2h^+ - y^+ & (h^+ \leq y^+ \leq 2h^+) \end{cases} \quad (6)$$

Table 2 Condition of wall.

	Flat	Non-slip	Slip 1	Slip 2
$A_{\max}^+$	0	6	6	6
wall	non-slip	non-slip	slip	slip
$u_{\text{wall}}^+$	0	0	$0.25u_{\tau}$	$0.50u_{\tau}$

### Wall conditions

Table 2 shows the conditions of amplitude and slip velocity. The amplitude of the wavy walls  $A$  was set equal to  $6\nu/u_{\tau}$ . Flow separation was not predicted because the ratio  $A/\lambda (=0.0127)$  was lower than the critical value of 0.02 (Tuan et al., 2006), over which the separation of flow occurs. Moreover, meandering flow was not predicted because the ratio of amplitude to the channel height ( $=2h$ ) was  $1/60$ . In the discussion below, the non-slip flat wall is referred to as Flat. The non-slip wavy wall is referred to as Non-slip ( $u = 0$ ). And the wavy walls with the slip velocity are referred to as Slip 1 ( $u = 0.25u_{\tau}$ ) and Slip 2 ( $u = 0.50u_{\tau}$ ).

In each case, the Reynolds number  $Re_{\tau} (=hu_{\tau}/\nu)$  was 180, where  $\nu$  is the kinematic viscosity and  $u_{\tau}$  is the friction velocity. Thus,  $u_{\tau}$  was unchanged in time and space. The Prandtl number was set to be 2.

### Spatiotemporal average statistics

In our study, we discuss the spatiotemporal average values over a plane normal to the  $y$ -axis in the period  $900 < t^+ < 4500$ . We confirmed that the temperature field and the flow field were developed at  $t^+ = 900$ . The fluctuating components of velocities and temperature were defined by the difference between a local instantaneous value and its spatiotemporal average value.

## RESULTS AND DISCUSSION

### Mean velocities

Figures 2 and 3 indicate the profiles of streamwise mean velocity. In the linear sub-layer, the mean velocity in the case of Slip 2 has the highest values compared with that in other cases, while the mean velocity in the case of Flat has the highest values in the buffer layer and log-law region. The mean velocity profile in Flat is in agreement with the profile obtained by Kawamura et al. (1998, 2000).

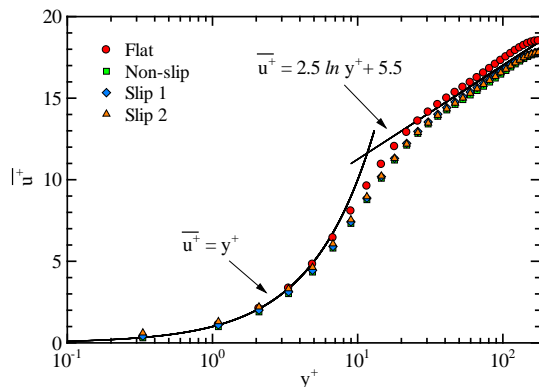


Fig. 2 Profiles of mean velocity.

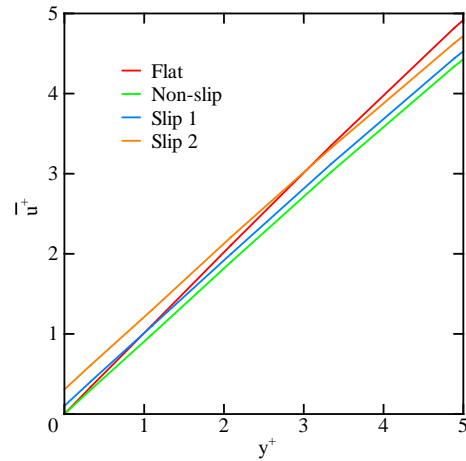


Fig. 3 Profiles of mean velocity in the linear sub-layer.

Table 3 Bulk mean velocity.

	Flat	Non-slip	Slip 1	Slip 2
$u_{\text{bulk}}^+$	13.13	12.53	12.63	12.70

The bulk mean velocity,  $u_{\text{bulk}}^+ = (1/2h) \int_0^{2h} \overline{u^+} dy^+$ , is shown in Table 3. In comparison with the case of Flat, it is found that the bulk mean velocity in the case of Non-slip decreased by 4.53% due to the wavy walls. Also, the bulk mean velocity in the case of Slip 1 and Slip 2 decreased by 3.77% and 3.24% due to the slip boundary conditions. The bulk mean velocity in the case of the wavy walls increased with an increase in the slip velocity.

### Turbulence intensities

Figure 4 indicates the profiles of turbulence intensities. We confirmed that the turbulence intensities in the case of Flat are in agreement with the predicted results obtained by Kawamura et al. (1998, 2000). The turbulence intensities in the case of the wavy walls are higher than those in the case of the flat wall in the linear sub-layer and the buffer layer, particularly in the case of the wavy walls with the slip velocity. The main flow is accelerated in the near-wall, uphill regions and is slightly decelerated in the near-wall, downhill regions. Thus, the mean velocity fluctuates regularly in the streamwise direction. This fluctuation causes an increase in the RMS values of fluctuating velocity. This is the reason for the increases in the turbulence intensities in the case of the wavy walls.

### Shear stresses

Figure 5 indicates the profiles of the viscous shear stresses and the Reynolds shear stresses. The viscous shear stresses in the case of the wavy walls are lower than those in the case of the flat wall in the region of  $y^+ < 10$ . There are not large differences in the viscous shear stress in the laminar sub-layer in the cases of the wavy walls. This is due to the fact that no difference is seen in the gradient of mean streamwise velocity in the sub-layer,

regardless of the type of slippery surface shown in Fig. 3. Therefore, the slip velocity of the wavy walls does not affect the viscous shear stress.

The Reynolds shear stresses in the case of the wavy walls are lower than those in the case of the flat wall in the region of  $y^+ < 20$ . Also, the Reynolds shear stresses in the case of the wavy walls take negative values in the region of  $y^+ < 10$ . The reason for the negative values of the Reynolds shear stresses is probably the enhancement of positive fluctuation velocities in the streamwise and wall-normal directions in the uphill regions of the wavy walls. The slip velocity does not affect the Reynolds shear stress in the buffer region, but slightly affects the stress in the linear sub-layer.

Table 4 shows the wall shear stress, which was defined by the sum of the viscous shear stress and the Reynolds shear stress at the adjacent grid to the surface. In comparison with the case of Flat, the wall shear stress in the case of the wavy wall is found to be 7.68%, 8.04% and 8.34% lower in the case of Non-slip, Slip 1 and Slip 2 respectively. The wall shear stress in the case of the wavy walls slightly decreases with an increase in the slip velocity.

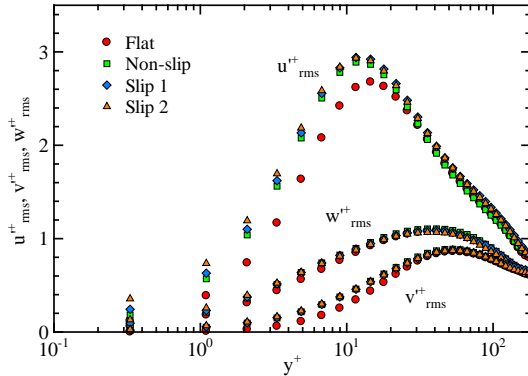


Fig. 4 Profiles of turbulence intensities.

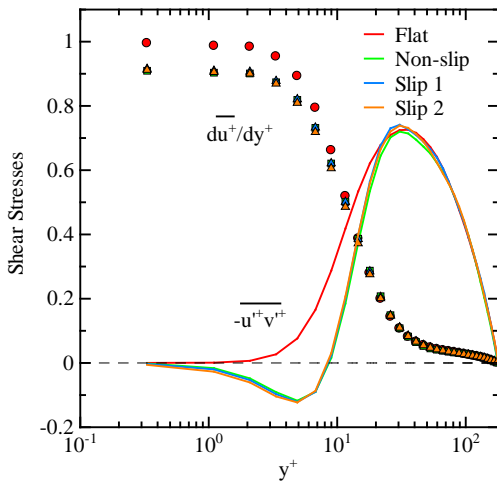


Fig. 5 Profiles of shear stresses.

Table 4 Wall shear stress.

wall shear stress	Flat	Non-slip	Slip 1	Slip 2
	0.999	0.922	0.919	0.916

### Mean temperature

Figures 6 and 7 indicate the profiles of mean temperature. The mean temperature in the case of Non-slip in the region of  $y^+ > 10$  is slightly lower than that in the case of Flat. Also, the mean temperatures in the case of Slip 1 and Slip 2 in the region of  $y^+ > 10$  are slightly lower than those in the case of Non-slip and Flat. The mean temperature in the wavy walls decreases with an increase in the slip velocity of the wavy wall.

Table 5 shows the bulk mean temperature  $\theta_{bulk}^+$ , where  $\theta_{bulk}^+ = (1/2h) \int_0^{2h} \overline{\theta^+} dy^+$ . The bulk mean temperature decreases with an increase in the slip velocity.

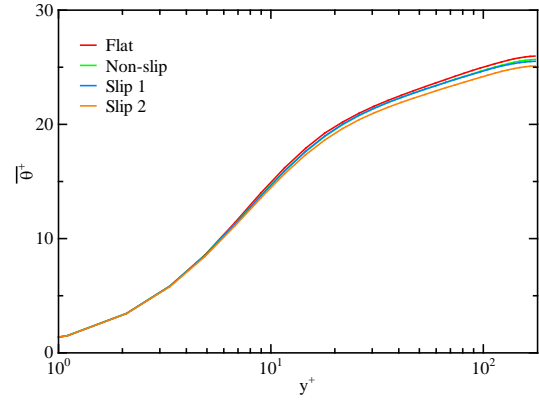


Fig. 6 Profiles of mean temperature.

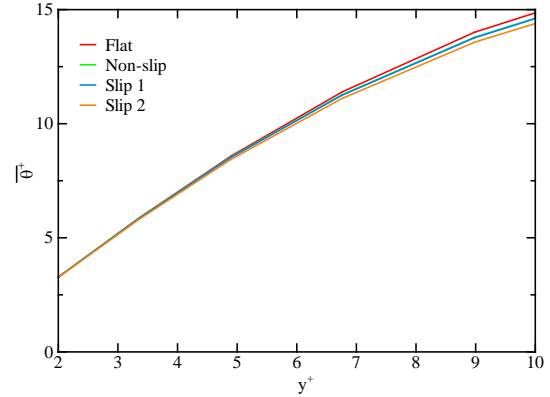


Fig. 7 Profiles of mean temperature in the linear sub-layer and the buffer region.

Table 5 Bulk mean temperature.

	Flat	Non-slip	Slip 1	Slip 2
$\theta_{bulk}^+$	19.64	19.43	19.39	19.04

## Nusselt number

Table 6 shows the mean Nusselt number. We calculated the mean Nusselt number from the profile of mean temperature. The mean Nusselt number is derived by the following equation (Kawamura, 1998).

$$Nu = 2 Re_\tau Pr / \int_0^{2h} \overline{\theta^+} dy^+ \quad (7)$$

The Nusselt number in the case of the wavy wall is 2.0%, 2.2% and 4.2% higher in the cases of Non-slip, Slip 1 and Slip 2 respectively than that in the case of Flat.

Table 6 Mean Nusselt number.

	Flat	Non-slip	Slip 1	Slip 2
$Nu$	36.66	37.38	37.45	38.16

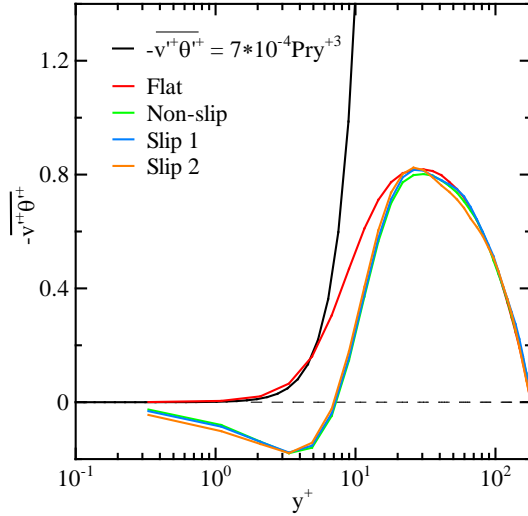


Fig. 8 Profiles of wall-normal turbulent heat flux.

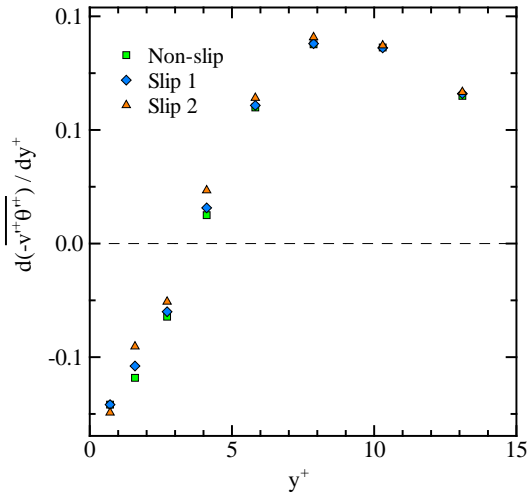


Fig. 9 Gradient of the turbulent heat flux ( $0 \leq y^+ < 15$ ).

## Turbulent heat flux

Figure 8 indicates the profiles of the wall-normal turbulent heat flux,  $-v^+ \theta^+$ , with an empirical equation (Antonia et al., 1991). In Fig. 8, the wall-normal turbulent heat flux takes positive values in the whole region in the case of the flat wall. On the other hand, it takes negative values in the region of  $y^+ < 8$  in the case of the wavy walls. In the region where the wall-normal turbulent heat flux takes negative values, the Reynolds shear stress also takes negative value in Fig. 5. Thus, in these specific regions, the velocity fluctuation of the wall normal direction contributes noticeably to the modification of the turbulent heat flux and the Reynolds shear stress. Furthermore, the similarity of the turbulent heat flux to the Reynolds shear stress is confirmed.

The values of wall-normal turbulent heat flux depend on the slip velocity. The wall-normal turbulent heat flux decreases with an increase in the slip velocity. This is due to the Reynolds analogy between the Reynolds shear stress and the wall-normal turbulent heat flux. On the other hand, the wall-normal turbulent heat flux in the buffer region increases with an increase in the slip velocity. This is slightly different from the dependency of the Reynolds shear stress in the region on the slip velocity. This is probably due to the difference between the effects on the fluctuating velocity of the slip condition for velocity and the effects on the fluctuating temperature of the non-slip condition for temperature.

The wall-normal turbulent heat flux in the case of the wavy walls recovers in the range of  $4 \leq y^+ < 20$ . The gradient of the turbulent heat flux is high in this range. Figure 9 indicates the profile of the gradient of the turbulent heat flux in the range of  $0 \leq y^+ < 15$  in the y-direction in the cases of the wavy walls. The higher the slip velocity, the higher the gradient of the turbulent heat flux is in the range of  $2 \leq y^+ < 7$ . This high gradient of the wall-normal turbulent heat flux contributes significantly to the diffusion term in the averaged energy equation. As a result, the mean temperature gradient decreases in the range. This is the reason for the low temperature values in the case of the slippery wavy walls shown in Fig. 7. This low temperature leads to the increase in the Nusselt number shown in Table 6.

## CONCLUSION

We carried out direct numerical simulation for turbulent flow in a channel whose heating walls are sinusoidal wavy-shaped. The ratio of amplitude and wavelength for the wavy wall was so low that the separation and reattachment for flow did not occur. Moreover, we have dealt with slippery surfaces. The main conclusions obtained are as follows:

(1) In the case of the wavy walls, the viscous stresses were reduced by the gentler velocity gradient in the near-wall region as compared with the case of the flat wall. It was found that there was no difference in the viscous stress by the slip conditions. As a result of the slight decrease in the Reynolds shear stresses in the near-wall region with an increase in the slip velocity, total shear stress slightly decreased.

(2) In the case of the wavy walls, the mean Nusselt number was found to be higher than that of the flat wall. Also, the mean Nusselt number increased with an increase in the slip velocity.

(3) The turbulent heat flux was found to take negative values in the linear sub-layer and the buffer region. The gradient of the turbulent heat flux in the buffer region increased with an increase in the slip velocity. This increase in the gradient of the turbulent heat flux leads to the gentler gradient of the mean temperature in the buffer region than that in the other cases. This is the reason for the lower bulk mean temperature and higher Nusselt number in the case of the wavy walls with the high slip velocity than that in the other cases.

## REFERENCES

Akaiwa, R., Nishida, A. and Hagiwara, Y., 2014, "Direct numerical simulation on the effects of amplitude and hydrophilicity of wavy wall on turbulent heat transfer and drag", *The 15<sup>th</sup> International Heat Transfer Conference*, 1-13.

Antonia, R. A. and Kim, J., 1991, "Turbulent Prandtl number in the near-wall region of a turbulent channel flow", *Int. J. Heat and Mass Transfer*, Vol. 34, 1905-1908.

Fujii, H., Sakurai, K., Nakano, T. and Hagiwara, Y., 2011, "Turbulence structure, friction drag and pressure drag due to turbulent flow over angled wavy surfaces", *Proc. of 7th Int. Symposium of Turbulence and Shear Flow Phenomena* (USB memory), 1-6.

Kader, B. A., 1981, "Temperature and concentration profiles in fully turbulent boundary layers", *Int. J. Heat and Mass Transfer*, Vol. 24, 1541-1544.

Kawamura, H. et al., 1998, "DNS of turbulent heat transfer in channel flow with low to medium-high Prandtl number fluid", *Int. J. of Heat and Fluid Flow*, Vol. 19, 482-491.

Kawamura, H., Abe, H., and Shingai, K., 2000, "DNS of turbulence and heat transport in a channel flow with different Reynolds and Prandtl numbers and boundary conditions", *3rd Int. Symp. on Turbulence, Heat and Mass Transfer*, 1-18.

Morinishi, Y., 1996, "Conservative properties of finite difference schemes for incompressible flow (2nd report, schemes in staggered and collocated grid systems)" (in Japanese), *Trans. Japan Soc. Mech. Eng. Ser B*, Vol. 62, pp. 4098-4105.

Tamura, A., Kikuchi, K. and Takahashi, K., 1997, "Residual cutting method for elliptic boundary value problems", *J. of Computational Physics*, Vol. 137, pp. 247-264.

Tuan, H., El-Sammi, O., Yoon, H.S. and Chun, H.H., 2006, "Immersed boundary method for simulating turbulent flow over a wavy channel", *Extended Abstracts of Whither Turbulence Prediction and Control*, pp. 116-117.

